Chemical Physics Letters 471 (2009) 239–243

Contents lists available at ScienceDirect

Chemical Physics Letters

journal homepage: www.elsevier.com/locate/cplett

Long-range interactions between polar molecules and metallic surfaces: A comparison of classical and density functional theory based models

Delia Fernández-Torre, Oona Kupiainen, Pekka Pyykkö, Lauri Halonen *

Department of Chemistry, University of Helsinki, P.O. Box 55 (A.I. Virtasen aukio 1), FIN-00014, Finland

ARTICLE INFO

Article history:
Received 11 December 2008
In final form 13 February 2009
Available online 20 February 2009

ABSTRACT

Long distance interactions of ammonia, hydrogen fluoride and water molecules adsorbed on a nickel (1 1 1) surface have been investigated using density functional theory (DFT) and a classical electrostatic model. The DFT approach uses periodic boundary conditions, the generalized gradient approximation and plane wave basis functions. In the classical approach, the molecules are treated as point dipoles and the metal surfaces are modelled using the image-charge method. The classical and DFT interaction energies agree well, and the image-charge method can thus be used as a simple description of interactions between molecules and metal surfaces.

1. Introduction

Understanding the interaction between a molecule and a metal surface is important for the study of various adsorption processes such as heterogeneous catalysis, molecular scattering from surfaces, desorption, diffusion and the aggregation and growth of molecular clusters and monolayers on surfaces. An accurate theoretical modelling of these interactions is challenging although a lot of work has already been done in this field [1–3]. The situation has changed in recent years because accurate electronic structure calculation methods have become available, eliminating the need to use adjustable empirical parameters [1,4]. Less accurate, computationally cheaper, approaches to deal with the same problem are semiempirical methods and mixed techniques (QM/MM methods), which treat the most relevant part of the system at a quantum mechanical level and the rest at a classical level [5,6].

The qualitative behavior of interaction potentials of molecules on metal surfaces is well known. The potential at short ranges, near the energy minimum, is dominated by orbital interactions, i.e. Pauli repulsion and covalent bonding, which require a quantum description. At longer distances, the main contributions come from electrostatic, induction and dispersion (van der Waals) interactions. The dispersion interactions arise from quantum electrodynamics, and must be calculated quantum chemically or using empirical methods [7–9]. In this work, we focus on the non-dispersive part of the long-range interactions, which can be treated approximately with a classical model.

Classically, interactions between metals and charged particles can be examined using the image-charge method. Furthermore, general charge distributions can be expanded in multipoles, whose interactions with metals can be evaluated using corresponding image multipoles. Some studies have used this approach to model metal or dielectric surfaces interacting with molecules, instead of employing a deeper microscopic approach [10–13]. As far as we know, however, the image-charge approach has never been tested against electronic structure calculations. This is the subject of the present work.

2. Electronic structure calculations

All electronic structure calculations were performed with the VASP 4.6 package [14], which uses density functional theory (DFT) and periodic boundary conditions (PBC). We employed the generalized gradient approximation (GGA) as parameterized by Perdew et al. [15]. The electronic wave functions were represented as linear combinations of plane waves, whose cut-off was set to 400 eV (1 eV = 0.1602177 aJ). The core electrons were described with the projector augmented plane wave (PAW) method. The convergence criterion for the electronic energy was chosen to be 5×10^{-5} eV and spin-unpolarized calculations were performed. We were interested in the energies of two types of systems: two molecules in a periodic cell, and a molecule on a Ni(1 1 1) surface. The slabs used to describe the surface were 6 Å thick and contained four metal layers. Convergence tests were run with five and six layers to check that the thickness of the metal slab did not affect the results significantly. The molecules were located on the top of a nickel atom in all cases, but tests were performed displacing the molecules along the surface plane. The results turned out to be independent of the adsorption site.

In computing the potential energy curves, we first relaxed separately the structures of the surfaces and the molecules in vacuum, keeping the unit cell parameters fixed and constraining the lowest layers of the surfaces (half of the total in all the cases) to their bulk

* Corresponding author.
E-mail address: lauri.halonen@helsinki.fi (L. Halonen).

0009-2614/$ - see front matter © 2009 Elsevier B.V. All rights reserved.
doi:10.1016/j.cplett.2009.02.037

positions. The structures were considered fully relaxed when the forces were smaller than 0.01 eV/Å (1 Å = 10^{-10} m). The molecule–molecule and the molecule–surface systems were constructed by keeping these geometries frozen. The interaction energies were evaluated for different distances between the molecules and the surfaces.

Detailed convergence tests are important, as we are exploring the long-range distances where the interaction energies are small, ranging from tens to a few meV. We selected the adsorption system with the NH_3 molecule situated at a distance of 6 Å over the Ni(1 1 1) surface, embedded in a periodic cell of $a = b = 7.5$ Å, $c = 18.6$ Å, $\alpha = \beta = 90°$ and $\gamma = 60°$, as a representative case to check the convergence. Tests were performed to find the optimal plane wave cut-off and $\boldsymbol{k}$-point sampling for a convergence of 1 meV in the potential energy. We found that a value of 400 meV for the cut-off energy and a $4 \times 4 \times 1$ Γ-centered Monkhorst-Pack mesh (corresponding to 10 irreducible $\boldsymbol{k}$-points) were adequate for our calculations. It was also found that the best choice to treat partial occupancies was a Methfessel-Paxton smearing of order 1 and a width of 0.1 eV for the relaxations and the tetrahedron method with Blöchl corrections for the energies. The inclusion of spin polarization significantly affected the total energies of both the nickel surface alone and the ammonia–nickel system, but lowered each almost by the same amount, approximately 2 eV. The interaction energies were decreased by only 2 meV and, therefore, spin-unpolarized calculations were sufficient for our purposes.

3. The classical electrostatic model

In the classical model, we treat molecules as point dipoles and metals as ideal conductors, and we calculate their interaction energies using the image-charge method.

The boundary condition for an electric field at the surface of a perfect conductor is such that the field must be perpendicular to the surface and vanish inside the conductor. In the case of a dipole above an infinitely wide flat metal surface, this boundary condition can be satisfied by replacing the metal by the mirror image of the dipole with respect to the surface, with the charges inverted. Above the surface, the field is identical in the two systems, so the energy of the dipole in the field above the metal is equal to its energy in the field of the image dipole.

The DFT calculations were performed in a periodic array consisting of metal sheets with layers of molecules between them. In a classical electrostatic treatment, however, electric fields cannot penetrate the metal slabs, and molecules interact only with the two nearest surfaces and with the other molecules of the same monolayer. The two metal surfaces can be modelled by an infinite array of image dipoles as in Fig. 1: each dipole (both real and image) has a mirror image with respect to both surfaces, so the boundary conditions are satisfied. The exact position of the classical surfaces with respect to the atoms of the DFT model remains an adjustable parameter.

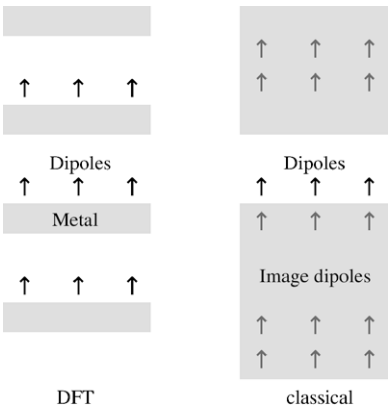

Fig. 1. Left: DFT model, right: corresponding classical model.

3.1. Electrostatic interaction energies in a periodic system

The electric field at the point r of a point dipole situated at the origin is

$$\boldsymbol{E}_{\mathrm{dip}}(\boldsymbol{r}) = -\frac{1}{4\pi\epsilon_0}\nabla\frac{\boldsymbol{\mu}\cdot\boldsymbol{r}}{r^3} = \frac{1}{4\pi\epsilon_0}\left(\frac{3(\boldsymbol{\mu}\cdot\boldsymbol{r})\boldsymbol{r}}{r^5} - \frac{\boldsymbol{\mu}}{r^3}\right), \tag{1}$$

where $\boldsymbol{\mu}$ is the dipole moment and ϵ_0 is the vacuum permittivity. The interaction energy of a point dipole at $\boldsymbol{r}_0$ with an external electric field $\boldsymbol{E}(\boldsymbol{r})$ is

$$U_{\mathrm{int}} = -\frac{1}{2}\boldsymbol{\mu}\cdot\boldsymbol{E}(\boldsymbol{r}_0). \tag{2}$$

Combining Eqs. (1) and (2), the energy of a dipole $\boldsymbol{\mu}_1$ in the field of an other dipole $\boldsymbol{\mu}_2$ is

$$U_{\mathrm{dip-dip}} = \frac{1}{8\pi\epsilon_0}\left(\frac{\boldsymbol{\mu}_1\cdot\boldsymbol{\mu}_2}{r_{12}^3} - \frac{3(\boldsymbol{\mu}_1\cdot\boldsymbol{r}_{12})(\boldsymbol{\mu}_2\cdot\boldsymbol{r}_{12})}{r_{12}^5}\right), \tag{3}$$

where $\boldsymbol{r}_{12}$ is the vector connecting the two dipoles and $|\boldsymbol{r}_{12}| = r_{12}$. If $\boldsymbol{\mu}_1$, $\boldsymbol{\mu}_2$ and $\boldsymbol{r}_{12}$ are all aligned, Eq. (3) reduces to

$$U_{\mathrm{dip-dip}} = -\frac{\mu_1\mu_2}{4\pi\epsilon_0 r_{12}^3}. \tag{4}$$

In our classical model, we have a cubic cell containing N molecules, which is repeated periodically in three directions. All the dipole moments have an equal magnitude μ and are oriented along the z axis. The interaction energy of one molecule at $\boldsymbol{r}_1 = \boldsymbol{0}$ with the field of the other molecules in this array is

$$U_{\mathrm{int,class}} = \frac{\mu^2}{8\pi\epsilon_0}\sum_{n_x=-\infty}^{\infty}\sum_{n_y=-\infty}^{\infty}\sum_{n_z=-\infty}^{\infty}\sum_{j=1}^{N}{}'\left(\frac{1}{|\boldsymbol{r}_j + L\boldsymbol{n}|^3} - \frac{3(z_j + Ln_z)^2}{|\boldsymbol{r}_j + L\boldsymbol{n}|^5}\right) \tag{5}$$

where $\boldsymbol{r}_j$ are the positions of the dipoles in the central cell, z_j are their z components, L is the length of the side of the cell, $L\boldsymbol{n} = L(n_x, n_y, n_z)$ are the vectors of the Bravais lattice corresponding to different periodic cells and the prime means that the term with $\boldsymbol{n} = \boldsymbol{0}, j = 1$ is omitted.

The sum in Eq. (5) does not converge absolutely, but it converges conditionally, i.e. it can have a finite value but the value depends on the summation order. A reasonable choice for the order is to start with the nearest cells and move outward in spherical shells, because the further away a molecule is, the better it would be shielded in a more realistic system of molecules with non-zero volume. However, the sum (5) converges too slowly to be practical. De Leeuw et al. [16] have evaluated (5) using the convergence factor $e^{-s|\boldsymbol{n}|^2}$ and performing the integration partly in reciprocal space. They found for it the expression

$$\begin{aligned}
U_{\mathrm{int,class}} = {} & \frac{\mu^2}{8\pi\epsilon_0}\sum_{j=2}^{N}\left\{\sum_{\boldsymbol{n}}\left[\mathrm{erfc}(\alpha|\boldsymbol{r}_j + L\boldsymbol{n}|)\left(\frac{|\boldsymbol{r}_j + L\boldsymbol{n}|^2 - 3(z_j + Ln_z)^2}{|\boldsymbol{r}_j + L\boldsymbol{n}|^5}\right)\right.\right. \\
& \left.\left. + \frac{2\alpha}{\sqrt{\pi}}\frac{\exp(-\alpha^2|\boldsymbol{r}_j + L\boldsymbol{n}|^2)}{|\boldsymbol{r}_j + L\boldsymbol{n}|^2}\left(1 - (z_j + Ln_z)^2\left(2\alpha^2 + \frac{3}{|\boldsymbol{r}_j + L\boldsymbol{n}|^2}\right)\right)\right] \right. \\
& \left. + \frac{4\pi}{L^3}\sum_{\boldsymbol{n}\neq\boldsymbol{0}}\frac{n_z^2}{|\boldsymbol{n}|^2}\exp\left(-\frac{\pi^2|\boldsymbol{n}|^2}{c^2\alpha^2}\right)\cos\left(\frac{2\pi}{c}\boldsymbol{n}\cdot\boldsymbol{r}_j\right)\right\} \\
\approx {} & \frac{\mu^2}{8\pi\epsilon_0}\sum_{j=2}^{N}\left\{\mathrm{erfc}(\alpha r_j)\left(\frac{r_j^2 - 3z_j^2}{r_j^5}\right) + \frac{2\alpha}{\sqrt{\pi}}\frac{\exp(-\alpha^2 r_j^2)}{r_j^2}\right. \\
& \left.\times\left(1 - z_j^2\left(2\alpha^2 + \frac{3}{r_j^2}\right)\right) + \frac{4\pi}{L^3}\sum_{n_x=-n_{\max}}^{n_{\max}}\sum_{n_y=-n_{\max}}^{n_{\max}}\sum_{n_z=-n_{\max}}^{n_{\max}}{}'\frac{n_z^2}{|\boldsymbol{n}|^2}\right. \\
& \left.\times\exp\left(-\frac{\pi^2|\boldsymbol{n}|^2}{c^2\alpha^2}\right)\cos\left(\frac{2\pi}{c}\boldsymbol{n}\cdot\boldsymbol{r}_j\right)\right\}
\end{aligned} \tag{6}$$

where erfc is the complementary error function

$$\mathrm{erfc}(x) = \frac{2}{\sqrt{\pi}} \int_x^\infty \mathrm{d}t e^{-t^2}. \quad (7)$$

The value of the parameter α is chosen so that the first sum over $\boldsymbol{n}$ can be truncated after the $\boldsymbol{n} = \boldsymbol{0}$ term and $n_{\max}$ is chosen so that the sum converges. The periodic images of the molecule whose energy is being calculated are excluded from the summation because interactions with them sum up to zero [16], and the prime means that the term with $\boldsymbol{n} = \boldsymbol{0}$ is omitted in the last sum.

The summation method used requires that the cells are cubic. In DFT adsorption calculations, cubic cells would make the calculations heavy, so instead in the classical model we employ cubic supercells containing several normal cells. We have adopted in all the classical calculations the experimental gas phase dipole moment values 1.82 D for hydrogen fluoride, 1.47 D for ammonia and 1.85 D for water [17] (1 D = 3.33564×10^{-30} Cm).

4. Interaction and adsorption energies

In the DFT model, the interaction energy (per molecule) of two molecules is calculated as

$$U_{\mathrm{int,DFT}} = \frac{1}{2} U_{2\text{ molecules per cell}} - U_{1\text{ molecule per cell}}. \quad (8)$$

In the classical model, the total interaction energy is the sum of individual dipole–dipole interaction energies, and (see Fig. 2) the equivalent of (8) reduces to

$$U_{\mathrm{int,class}} = U_{\text{interaction with other molecule and its periodic images}}. \quad (9)$$

The adsorption energy on a metal surface is, in the DFT model,

$$U_{\mathrm{ads,DFT}} = U_{\mathrm{metal+molecule}} - U_{\mathrm{metal}} - U_{\mathrm{molecule}}. \quad (10)$$

In the classical model, the cell with the molecule and its mirror image has a different height from the initial cell (see Fig. 1). The adsorption energy is now

$$U_{\mathrm{ads,class}} = U_{\text{interaction with all molecules, new cell}} - U_{\text{interaction with own periodic images, initial cell}}. \quad (11)$$

5. Results and discussion

5.1. Two molecules in a periodic arrangement

We first test our classical model with a system consisting of two periodically repeated polar molecules, instead of a molecule and a metal surface. We consider HF molecules in two different cells, C1 and C2, whose parameters are presented in Table 1, and NH_3 molecules in the smaller hexagonal cell, C2.

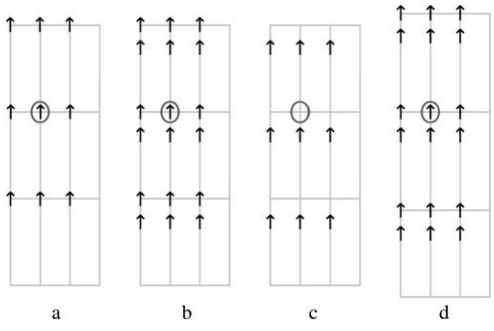

Fig. 2. (a) One molecule (encircled) interacting with its own periodic images. (b) The encircled molecule interacting with another molecule and the periodic images of both. (c) The classical equivalent of a PBC DFT interaction energy of two molecules is the dipole–dipole interaction energy of the encircled molecule with the other molecule and its periodic images. (d) In the classical model of the adsorption system, the cell height is different from that in the initial cell.

Table 1
Cell parameters: a, b and c are the cell dimensions, γ is the angle between a and b (the other angles are $\alpha = \beta = 90°$), and n_x, n_y and n_z give the number of cells contained in the supercell of the classical model in each direction.

		a (Å)	b (Å)	c (Å)	γ (°)	n_x	n_y	n_z
Cell C1	DFT	15.00	15.00	30.00	90			
	Classical	15.00	15.00	30.00	90	2	2	1
Cell C2	DFT	7.49	7.49	18.61	60			
	Classical	7.43	7.57	18.58	60.5	30	34	12

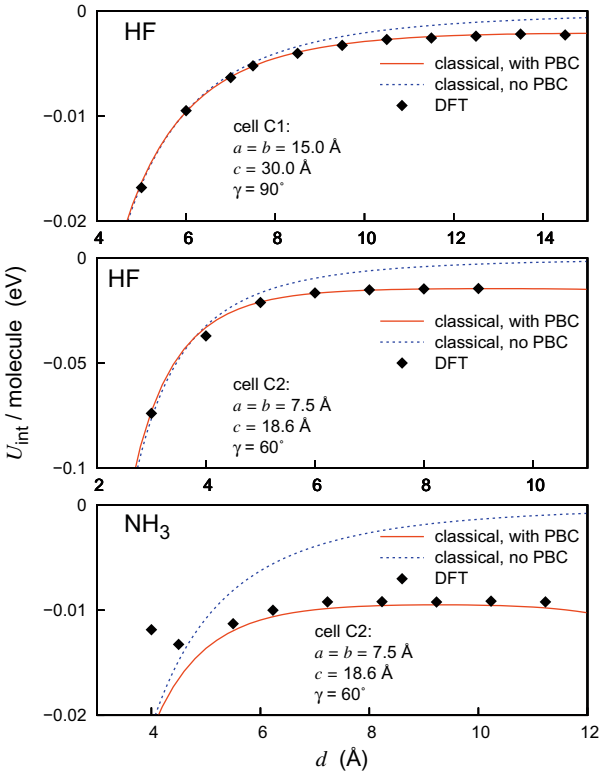

Fig. 3. The interaction energy of two HF or NH_3 molecules.

The DFT and classical interaction energies (Eqs. (8) and (9)) are presented in Fig. 3. We have also included the classical interaction energy of two dipoles without periodic boundary conditions (Eq. (4)).

In all three cases, the DFT and classical PBC energies agree well at long distances. For the HF molecules, the agreement is good even at an intermolecular distance of 3 Å, while for the NH_3 molecules, short-range interactions are important up to ca. 5 Å.

The non-PBC model works at short distances (less than ~1/4 of the cell height), but fails to give the right limit at long distances. Therefore, periodical boundary conditions have to be included in the classical model, if a sensible comparison with PBC DFT calculations is required.

5.2. Adsorption on the Ni(1 1 1) surface

We have investigated the long distance interactions of HF, NH_3 and H_2O on the Ni(1 1 1) surface in two cells whose lattice parameters are presented in Table 2.

Table 2
Cell parameters: Δh is the thickness of the surface, a, b and c are the cell dimensions, γ is the angle between a and b (the other angles are 90°), and n_x, n_y and n_z give the number of cells contained in the supercell of the classical model in each direction.

		Δh (Å)	a (Å)	b (Å)	c (Å)	γ (°)	n_x	n_y	n_z
Cell C2	DFT		7.49	7.49	18.61	60.0			
	Classical	2.09	7.54	7.46	16.96	59.7	36	21	16
		2.58	7.50	7.50	14.99	60.0	26	15	13
		2.76	7.51	7.49	14.27	59.9	19	11	10
Cell C3	DFT		7.49	7.49	28.61	60.0			
	Classical	1.62	7.52	7.48	38.86	59.9	31	18	6
		2.85	7.54	7.46	33.92	59.7	36	21	8

In the classical calculations, the distance between a molecule and its mirror image, and thus their interaction energy, depend on the location of the mirror plane. Furthermore, the distance between the two opposite mirror planes affects the height of the periodic cell (Fig. 4). The surface of a metal slab, however, is not well-defined on a microscopic scale, as can be seen in Fig. 5. Instead, the charge density decreases gradually between 1 and 3 Å above the centers of the topmost atoms.

We have tried several thicknesses for the surface layer, measured from the centers of the topmost Ni atoms to the mirror plane. The cell parameters for these systems are presented in Table 2. The classical and DFT adsorption energies (Eqs. (10) and (11)) are presented in Fig. 6.

The DFT energies do not agree perfectly with any of the classical energy curves for distances smaller than ca. 6 Å. The overall shape of the curves is similar, however, and the long distance limit in the DFT calculations is predicted well with the classical model using a surface thickness of ca. 2.5 Å.

All the energy differences between classical and DFT results are of the order of a few millielectronvolts, which is comparable to the accuracy of our DFT calculations. The differences could be due to several things: remaining short-range orbital interaction, change in the dipole moment or shifting of the surface due to induction or charge transfer, inaccuracy of the DFT calculations, or simply the assumption that the metal can be treated as a perfect conductor with a clear cut surface even at such small scales.

The good agreement at $h > 7$ Å in the larger cell suggests that the non-dispersive part of long-range adsorption interactions is well approximated by a classical dipole-conductor interaction. In a real adsorption system with only one metal surface, a simpler model with periodicity in just two dimensions could then be used to get the right asymptotic behavior. In that case, the convergence problem would also be avoided.

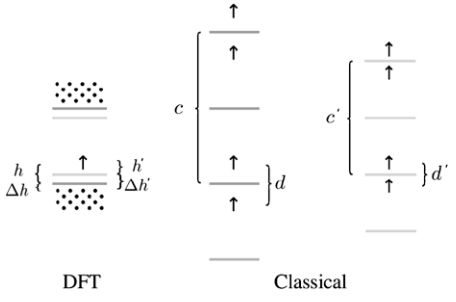

Fig. 4. Depending on where the classical surface is situated compared to the metal atoms of the DFT model, i.e. what the distance Δh between the topmost atoms and the mirror plane is, the classical model has a different cell height c and a different intermolecular distance d.

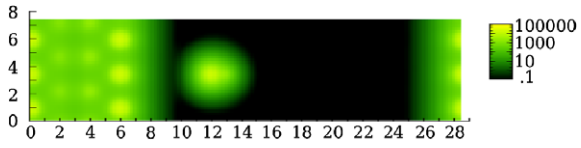

Fig. 5. Electron density (arbitrary units) of an HF molecule on a Ni(1 1 1) surface.

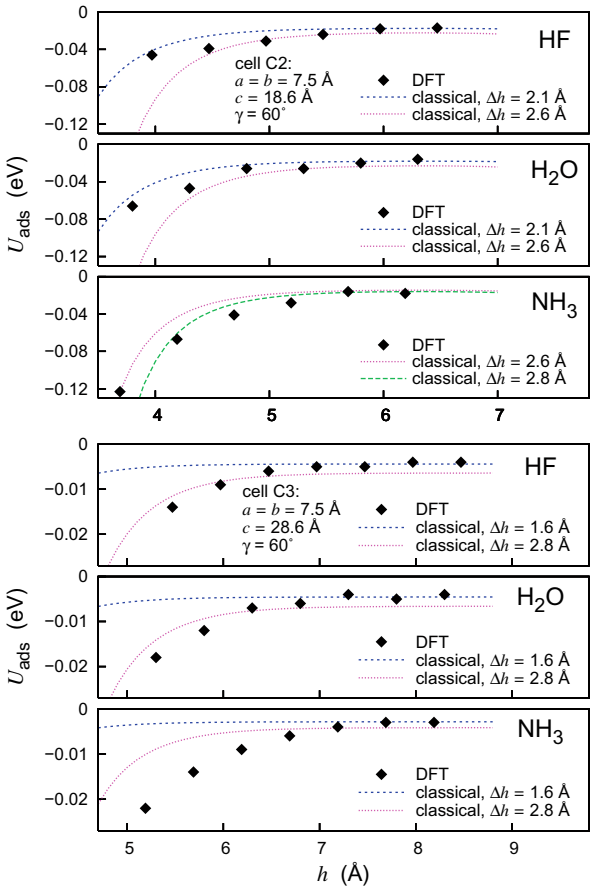

Fig. 6. Adsorption energies of H_2O, HF and NH_3 molecules on the Ni(1 1 1) surface in the cells C2 and C3 with different classical surface thicknesses Δh.

6. Conclusions

We have investigated interactions between molecules and metal surfaces using both DFT and classical models. At short distances, such interactions must be treated quantum mechanically, but further away they are believed to reduce to more simple dispersion forces and classical Coulomb type interactions. The aim of this contribution is to gain deeper understanding of quantum mechanical results at long distances, and how well they can be approximated with non-quantum mechanical approaches. Since the density

functional theory we have used does not include long-range dispersion interactions, we have only compared it with classical electrostatic interactions.

We have assumed, in our classical model, that dipolar molecules can be treated as point dipoles. We have investigated the validity of this approximation by comparing DFT and classical dipole–dipole interaction energies in periodic arrays of hydrogen fluoride molecules and of ammonia molecules. The agreement between these two approaches turns out to be excellent: for the HF molecules with a bond length of $r_{HF} = 0.94$ Å, the classical point dipole approximation works perfectly even when the distance between the centers of mass of two molecules is only 3 Å, and also for the less point-like ammonia molecules it works down to an intermolecular distance of 5 Å.

The four atom layer thick metal slabs have been treated as ideal conductors with zero resistivity and a well-defined flat surface. The interactions between molecules and surfaces have then been studied using the image-charge method. A significant issue in this approach is how to define the location of the surface, since the charge density decreases gradually in a region from the last metal layer to ca. 3 Å above it. We have calculated classical interaction potentials for different choices of the height of the classical surface ranging from 1 to 3 Å above the topmost metal atoms, and compared them with DFT calculations in systems consisting of a Ni(1 1 1) surface and either HF, water or ammonia molecules. None of the classical curves agree perfectly with DFT results in any of the systems. At long distances, however, the DFT energies approach the classical potential with a surface height of ca. 1.5–2 Å. Even at shorter distances, the differences between classical and DFT results are usually less than 10 meV. We thus conclude that the comparison of classical interaction potentials to *ab initio* results provides a way to define the classical surface of a metal at a microscopic scale and, furthermore, once this surface is defined, the long-range electrostatic interaction between molecules and metals can be approximated by means of a simple image-charge model.

Acknowledgements

The authors wish to thank the Academy of Finland and the University of Helsinki for financial support. We belong to the Finnish CoE in Computational Molecular Science. The CSC Ltd., Espoo, is thanked for the computer time.

References

[1] G.P. Brivio, M.I. Trioni, Rev. Mod. Phys. 71 (1999) 231.
[2] G.-J. Kroes, A. Gross, E.-J. Baerends, M. Scheffler, D.A. McCormack, Acc. Chem. Res. 35 (2002) 193.
[3] G. Lanzani, R. Martinazzo, G. Materzanini, I. Pino, G.F. Tantardini, Theor. Chem. Acc. 117 (2007) 805.
[4] J.R. Reimers, Z.-L. Cai, A. Bilic, N.S. Hush, Ann. N.Y. Acad. Sci. 1006 (2003) 235.
[5] Y. Okuno, T. Yokoyama, S. Yokoyama, T. Kamikado, S. Mashiko, J. Am. Chem. Soc. 124 (2002) 7218.
[6] T. Sumi, Y. Sakai, Phys. Rev. B 55 (1997) 4755.
[7] M. Elstner, P. Hobza, T. Frauenheim, S. Suhai, E. Kaxiras, J. Chem. Phys. 114 (2001) 5149.
[8] S. Grimme, J. Comp. Chem. 27 (2006) 1787.
[9] J.P. Jalkanen, M. Halonen, D. Fernández-Torre, K. Laasonen, L. Halonen, J. Phys. Chem. A 111 (2007) 12317.
[10] I.V. Ionova, S.I. Ionov, R.B. Bernstein, J. Phys. Chem. 95 (1991) 8371.
[11] B.L. Maschhoff, J.P. Cowin, J. Chem. Phys. 101 (1994) 8138.
[12] I. Panas, J. Mol. Struct. 388 (1996) 169.
[13] Y. Okuno, S. Mashiko, Thin Solid Films 499 (2006) 73.
[14] G. Kresse, J. Furthmüller, Phys. Rev. B 54 (1996) 11169.
[15] J.P. Perdew, J.A. Chevary, S.H. Vosko, K.A. Jackson, M.R. Pederson, D.J. Singh, C. Fiolhais, Phys. Rev. B 46 (1992) 6671;
J.P. Perdew, J.A. Chevary, S.H. Vosko, K.A. Jackson, M.R. Pederson, D.J. Singh, C. Fiolhais, Phys. Rev. B 48 (1993) 4978.
[16] S.W. de Leeuw, J.W. Perram, E.R. Smith, Proc. R. Soc. Lond. A 373 (1980) 27.
[17] C.L. Yaws, Chemical Properties Handbook, McGraw-Hill, New York, 1999.